



Influence of post-casting treatments on sulphonated polyetheretherketone composite membranes

Alessandra Carbone^{a,*}, Irene Gatto^a, Akihiro Ohira^b, Libin Wu^b, Enza Passalacqua^a

^a CNR-ITAE, Institute for Advanced Energy Technologies "N. Giordano" Via Salita S. Lucia sopra Contesse, 5 – Messina, Italy

^b FC-CUBIC (Polymer Electrolyte Fuel Cell Cutting-Edge Research Center) AIST Tokyo Waterfront, 2-41-6, Aomi, Koto-ku, Tokyo 135-0064, Japan

ARTICLE INFO

Article history:

Received 16 October 2009

Received in revised form

18 December 2009

Accepted 16 February 2010

Available online 20 February 2010

Keywords:

Composite s-PEEK membranes

Functionalised silica

Post-casting treatments

Freezable water

PEFC

ABSTRACT

Since the post-casting treatments influence the water entrapped in polymeric matrix and consequently its proton conductivity, an evaluation of annealing at 200 °C and acid treatments was conducted on previously developed composite s-PEEK (1.55 mequiv. g⁻¹) membranes, containing a commercial aminopropyl-functionalised silica. DSC, WAXS, SEM-EDX and laser microscope measurements carried out on membranes swollen at different temperatures highlighted different membrane properties depending on post-casting treatments. It was found that composite membranes have different structural and morphological characteristics than pristine polymer membranes. The silica distribution was modified when different treatments are used. The state of water changed when silica was inserted into the membranes. Actually, contrary to the pristine membranes the presence of freezable water was revealed at temperature lower than 80 °C. The proton conductivity was also affected by the presence and the amount of water trapped into the membranes and was particularly influenced by the post-casting treatments. The silica introduction reduced the swelling effect and improved the robustness of the membranes even if a higher water content in the freezable state was observed. Acid treatment leads to significant improvement in membrane properties, but the present work shows that annealing before acid treatment can affect the membrane morphology more strongly than other treatments resulting in a much better fuel cell performance.

© 2010 Elsevier B.V. All rights reserved.

1. Introduction

Composite membranes are considered as a valid choice as an electrolyte for medium temperature Polymer Electrolyte Fuel Cells (PEFCs). When used in PEFC and especially for application in the automotive field, the challenge is to operate at temperature above 100 °C reducing gases pressure and humidification keeping a high proton conductivity [1,2]. An additional challenge is to reduce production costs of fuel cell components and then, research efforts are concentrated on the development of non-noble metals or alloys as electrocatalysts and a low-cost membranes based on non-perfluorinated polymers. The development of poly-aromatic membranes plays a key role because Nafion[®] membranes are, until now, the most widely used [3–8,13]. Important literature has been dedicated on this class of polyelectrolyte but some problems are still to be overcome such as low proton conductivity at reduced relative humidity, weak mechanical stability and short lifetime. One of the most used polymer membrane is based on sulphonated polyetheretherketone (s-PEEK) with a sulphonation degree in the

range of 40–60%. Its excessive swelling when temperatures higher than 80 °C are used, produces a drop of mechanical properties and a reduction of its lifetime. On the contrary, the swelling effect is directly related to the proton conductivity increase due to the introduction of freezable water into the polymeric matrix [8]. In this context, inorganic/organic composite membranes have very interesting features as far as water balance is concerned since the inserted inorganic compound both acts as a mechanical reinforcement and as an additive hydrophilic agent [9–12]. The inorganic component might, but not necessarily, present intrinsic proton-conduction properties: in this case the solid will be acidic. In other cases, for example, with silica, titania or zirconia, the inorganic component is not inherently proton-conducting and is used as water-retaining inorganic filler or as a mechanical support. The properties of these composite membranes not only depend on the nature of the ionomer and the solid used, but also on the amount, the homogeneous dispersion, the size and the orientation of the solid particles dispersed in the polymeric matrix that can provide additional pathways for proton conduction [14–19].

Currently, the research is moving towards the development of membranes containing nitrogenous groups that promote the acid–base interaction between functional groups NH–SO₃H [20,7]. Actually, the sulphonic acid groups interact with the nitrogenous

* Corresponding author. Tel.: +39 090 624 240; fax: +39 090 624 247.
E-mail address: carbone@itae.cnr.it (A. Carbone).

Table 1
Membranes post-casting treatments.

Membrane name	Polymer	Silica %	Treatments
A	s-PEEK	0	HCl
B			H ₂ SO ₄
C			H ₂ SO ₄ + 200 °C
D			200 °C + H ₂ SO ₄
SiONH-A	s-PEEK	20%wt	HCl
SiONH-B			H ₂ SO ₄
SiONH-C			H ₂ SO ₄ + 200 °C
SiONH-D			200 °C + H ₂ SO ₄

base by forming hydrogen bridges, protonation of the nitrogen sites and polysalts formation and then the proton conductivity is improved. In this context, composite s-PEEK membranes containing an aminopropyl-functionalised silica gel (SiO–NH₂) were developed in a previous work [21] resulting in an improved mechanical resistance and proton conduction. In the SiO–NH₂ membrane, the interactions between the sulphonic groups of the polymers and the aminic groups of the silica limit the swelling phenomena at critical temperatures and improve the mechanical properties. Since the post-casting treatments influence the water entrapped in the polymeric matrix acting on the polymer structure, it was judged fundamental to understand how the annealing and acid treatments can control the inorganic/organic interactions.

In this work, several post-casting treatments were performed on previously developed composite membranes to investigate the behaviour of water content (freezable and unfreezable), morphological properties, proton conductivity and electrochemical performance.

2. Experimental

2.1. Membranes preparation

Composite membranes were prepared starting from a dispersion of sulphonated polyetheretherketone (s-PEEK, IEC = 1.55 mequiv. g⁻¹) in DMAc as ionomer and a 20% (wt/wt) of a commercial 3-aminopropyl-functionalised silica gel (Aldrich, ~1 mmol g⁻¹ NH₂ loading), as reported in a previous paper [21]. All samples were treated at 120 °C for 15 h before each treatment. Post-casting treatments were performed on dried membranes in terms of annealing (200 °C, 30 min) and acid treatments (HCl 1 M at r.T. for 1 h or H₂SO₄ 1 M at 80 °C for 2 h followed by rinsing in water), as described in Table 1.

2.2. MEAs preparation

Home-made electrodes were prepared by a spray technique described in the referenced paper [22] and coupled to the membranes to obtain MEAs. The same Pt loading (0.5 mg cm⁻²) in the catalytic layer was used for both anodes and cathodes and a 30% Pt/Vulcan (E-Tek Inc.) was used as an electrocatalyst.

2.3. Membranes characterisations

2.3.1. Water uptake measurements

The water uptake (w.u.) data were calculated from the difference in weight of the dried and the wetted samples. The dry mass was obtained after a desiccation of the sample in an oven under vacuum (1000 mbar) for 2 h, while the wet mass was obtained after the immersion in water at 24 °C, 40 °C and 80 °C for 2 h of the dried samples.

2.3.2. DSC measurements

The wet samples were punched into wafer of about 3.5 mm diameter and sealed in aluminium pans to keep the constant water uptakes. The calorimetry was performed using DSC-60 (Shimadzu, Japan) over a range of –100 °C to 20 °C at a scanning rate of 5 °C min⁻¹ with liquid nitrogen as a refrigerant. DSC-60 has a nitrogen-purged sample chamber with a temperature accuracy of ±0.01 °C. An empty Al sealed pan was used as a reference. Thermograms were recorded as samples were cooled from 20 °C to ~–100 °C at first, and then heated from –80 °C to 20 °C.

2.3.3. X-ray analyses (WAXS)

The X-ray powder diffraction (WAXS) analyses were performed by using a Rigaku Ultima-IV X-ray diffractometer with Ni-filtered CuKα radiation (λ = 0.15418 nm) operated at 40 kV and 40 mA in air, in the symmetrical reflection mode. Samples were scanned under diffraction angle in the 2θ range of 5–90° with a step scan interval of 0.5° min⁻¹. The profiles were smoothed and background (dark scattering) was subtracted.

2.3.4. Laser microscopy analyses

A confocal laser microscope (nano search microscope SFT 3500, Shimadzu, Japan) equipped with semiconductor laser (λ = 408 nm) was used to investigate the macroscopic morphology of the membranes and the silica distribution in composite membranes.

2.3.5. SEM–EDX analyses

A field emission Scanning Electron Microscope equipped with EDAX microprobe (Philips mod. XL30 S FEG) was used to obtain the surface morphology of the membranes. A colloid graphite aqueous base (TAAB) was used to fix the sample on the stab and graphite coating was used to avoid sample charring.

EDX measurements were carried out to investigate the Si distribution in composite membranes using the K lines. The mapped surface is of about 20 μm × 10 μm and the used mapping matrix had a dimension of 256 × 200.

2.3.6. Proton conductivity measurements

The membrane proton conductivity was measured in the longitudinal direction as a function of temperature (from 30 °C to 80 °C) and relative humidity of 100%RH, as described elsewhere [21].

2.3.7. Fuel cell tests

Fuel cell tests, in terms of polarisation curves, were carried out in a commercial 25 cm² single cell in a temperature range 80–120 °C, with humidified H₂ and air at 3 absolute Bars. The gas fluxes were fixed at 1.5 and 2 times the stoichiometry at a current density of 1 A cm⁻² for hydrogen and air, respectively.

3. Results and discussion

All prepared samples (Table 1), previously wetted at 24 °C, 40 °C and 80 °C, were characterised in terms of DSC measurements in order to determine the amount of water, both freezable (F) and unfreezable (UF). The water fraction of pure s-PEEK as a function of the treatments and temperature is reported in Fig. 1.

Until 40 °C, the total water content is UF for each post-casting treatment meaning that the amount of adsorbed water is strongly coordinated to the sulphonic groups and is unavailable to freeze at temperature below 0 °C. Its amount is ruled from the sulphuric acid treatment following this order: A < C < B < D. The sulphuric acid improves the wettability and consequently the membranes that underwent this treatment as the last step (B and D) show the highest UF content. Above 80 °C, the polymeric matrix is able to entrap more water due to the beginning of the swelling process, then F water is present. The wettability in terms of total amount of water

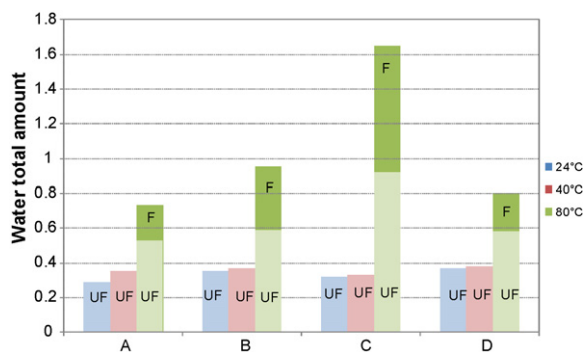


Fig. 1. s-PEEK membranes water fraction as a function of treatments and temperature.

increases when H_2SO_4 (B) is used instead of HCl (A), but a further annealing on H_2SO_4 treated sample (C) produces a massive water adsorption due to a weakening of the polymeric structure caused by acid. As far as the F and UF water fractions, the same trend of total water fraction is observed for sample A, B and C. However annealing before acid treatment (D) does not affect the UF water content and constrains the polymer structure limiting the amount of F water.

In composite s-PEEK–SiONH₂ membranes the total amount of water is lower than s-PEEK (Fig. 2), due to interactions between NH₂–SO₃H groups [21] that reduce the polymer capability to coordinate water.

Contrary to pristine polymer, the F water is already present at $T < 80^\circ C$ and it is quite constant for each sample below $80^\circ C$. This is a consequence of the introduction of the same amount of silica (20% wt/wt) into the membranes that incorporates water into its pores in a phase free to freeze [24].

At $80^\circ C$, the swelling effect is predominant and the polymer matrix plays a key role. The behaviour is comparable to pristine polymer membranes ($A < B < C$). In particular, in sample C the excessive amount of F water is due to the annealing as last step that not only destabilises the polymer matrix but breaks all the beneficial interactions between polymer and silica [21]. The optimal situation was found in sample D where the concomitant effect of post-casting treatments and functionalised silica presence is responsible for both the good stability of the polymer structure and the low swelling.

The influence of the post-casting treatments on the polymer structure was investigated through WAXS analyses. In Fig. 3 the membranes profiles that underwent treatments A, C and D are shown.

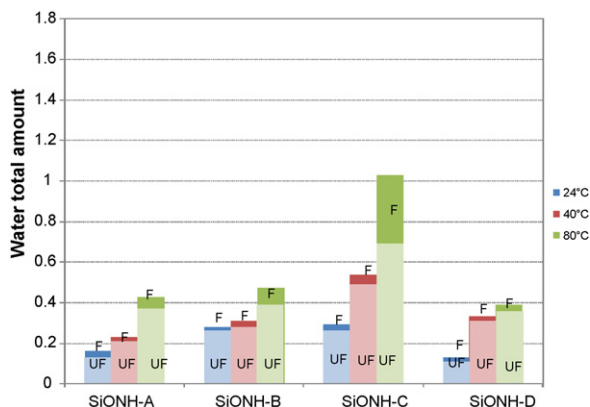


Fig. 2. Composite membranes water fraction as a function of treatments and temperature.

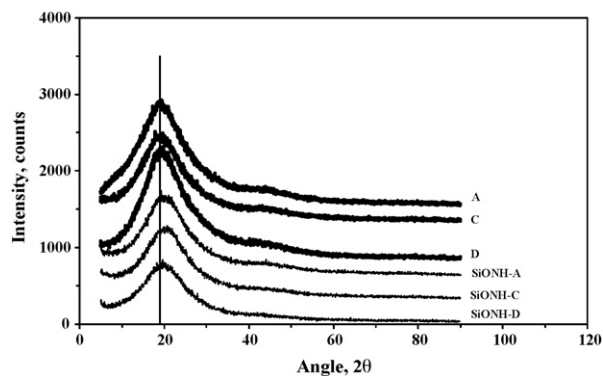


Fig. 3. Pure and composite s-PEEK membranes WAXS analyses comparison.

Whatever is the post-casting treatment the pristine s-PEEK samples present a peak at $2\theta = 18.9^\circ$, corresponding to crystalline phase (1 1 0) which is overlapped on a broad amorphous phase [23,25]. However, the peak profile (peak intensity and FWHM) differs from each other. The peak intensity of sample D is higher and the peak profile is sharper than those of the other membranes. The annealing over the glass transition ($T_g: 142^\circ C$ [26]) gives a slight improvement in crystallinity. This result clearly shows that annealing before acid treatment affects the morphological change leading in increment in crystallinity and resulting in the suppression of dimensional change by swelling.

For composite membranes the introduction of SiO–NH₂ decreases the crystallinity. The peaks are shifted towards higher 2θ values and lower intensity than pure s-PEEK. In particular the 2θ values are 19.5, 19.5 and 19.1 for sample A, C and D, respectively.

Krishnan et al. [25] have reported similar characteristics showing a s-PEEK composite membrane with boron phosphate prepared by in situ sol–gel process reduces the crystallinity compared to pure s-PEEK membrane.

Laser microscopy on composite membranes surface was carried out to verify the membrane morphology, as reported in Fig. 4.

At low magnification (scan size $1280 \mu m \times 960 \mu m$), it is possible to observe that the morphology changes with the post-casting treatment. The bright area corresponds to agglomerates of silica and dark area might correspond to polymer matrix and dispersed silica. For samples A and C, the silica is regularly dispersed (dark area) and arises agglomerates (bright area), with macroscopic dimensions, probably positioned in the vicinity of the hydrophilic domains of the polymer. For sample C, agglomerates are smaller than those in sample B. This implies that annealing after acid treatment affects the macroscopic morphological change by reducing the interactions between polymer matrix and silica phase. This is revealed by the incorporation of the highest amount of water (see Fig. 2). In samples B and D, the morphology is similar but differs from the others. The silica distribution is regular but the agglomerates dimension is higher than that for other samples. Because the laser microscope has a magnification in the macroscale, the morphological profile was also verified by SEM analyses. At low magnification, comparable to Laser scans, a phase separation between polymer and silica was observed, as reported in Fig. 5 for samples B and C and are in accordance with laser microscope analyses.

At high magnifications, a dense and compact structure was observed for all analysed samples.

In order to verify the silica dispersion into the membranes, EDX mapping on Si element were affected on two regions of composite membranes, one rich in polymer (polymer fraction) and the other one rich in silica (silica fraction), as reported in Fig. 6.

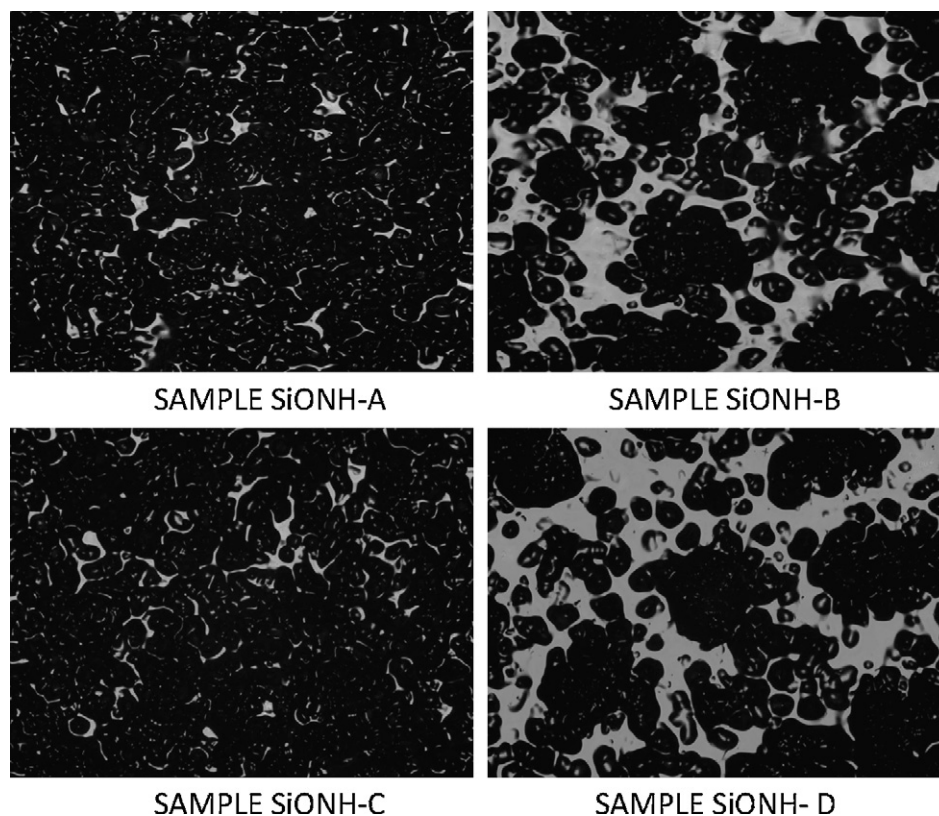


Fig. 4. s-PEEK-SiONH membranes laser microscope images at 5 \times magnification

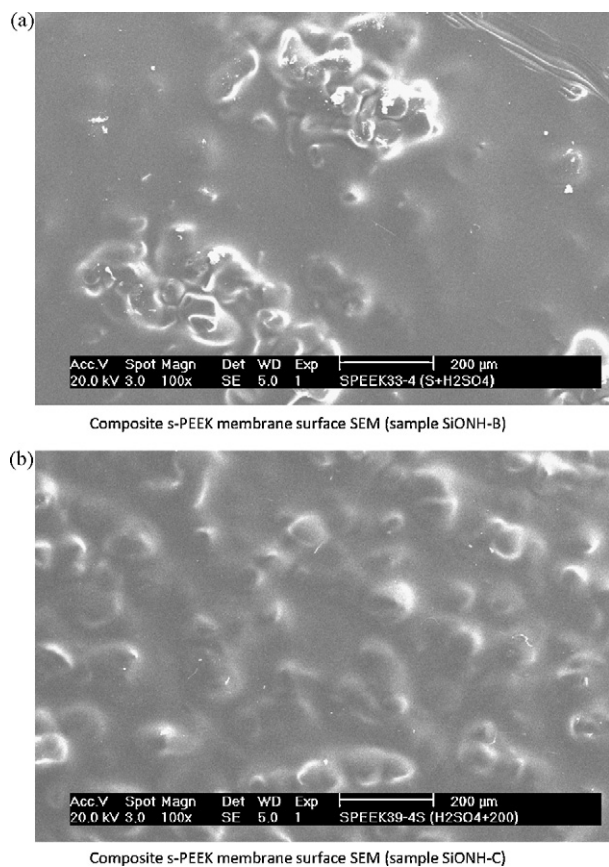


Fig. 5. SEM analyses on surface of (a) composite membrane B-treated and (b) composite membrane C-treated at low magnifications.

A well-dispersed Si can be seen in polymer fraction, meaning that silica is homogeneously distributed in polymer matrix in the micro-scale. Only the pictures related to sample SiONH-D are shown but, in any case, all samples present the same silicon distribution.

Membranes proton conductivity, in the longitudinal direction, was measured as a function of the swelling temperature and compared to F water for pristine and composite membranes, as reported in Figs. 7 and 8, respectively.

For pristine s-PEEK samples (Fig. 7) the conductivity increases by increasing the temperature and reaches the highest values when F water is present (80 °C).

Even if the sample C presents the highest F water content the proton conductivity has not the same trend. An excessive swelling due to the treatment provokes a drop of mechanical properties influencing the proton conduction.

SiONH samples (Fig. 8) show a conductivity lower than pristine membranes. At $T < 80$ °C the conductivity follows the trend $C < A < B < D$. This behaviour is due to an additive interaction between H_2SO_4 and NH_2 when H_2SO_4 is the last treatment (B and D) that enhances the conductivity; the annealing at 200 °C as last treatment (C) breaks down all the interactions reducing the conductivity and HCl treatment (A) does not produce any additive effect on proton conduction. For samples A, B and D, wherein F water was found at all temperatures, the conductivity follows a linear trend with the temperature increase. While the sample C presents the highest amount of F water in the whole investigated temperature range, the proton conductivity does not follow the same trend, as observed for pristine membrane. In any case at 80 °C, similar values are reached due to the swelling effect of the polymer matrix that is predominant at this temperature.

To verify the electrochemical behaviour in a fuel cell device, polarisation curves at 80 °C and 120 °C were carried out comparing

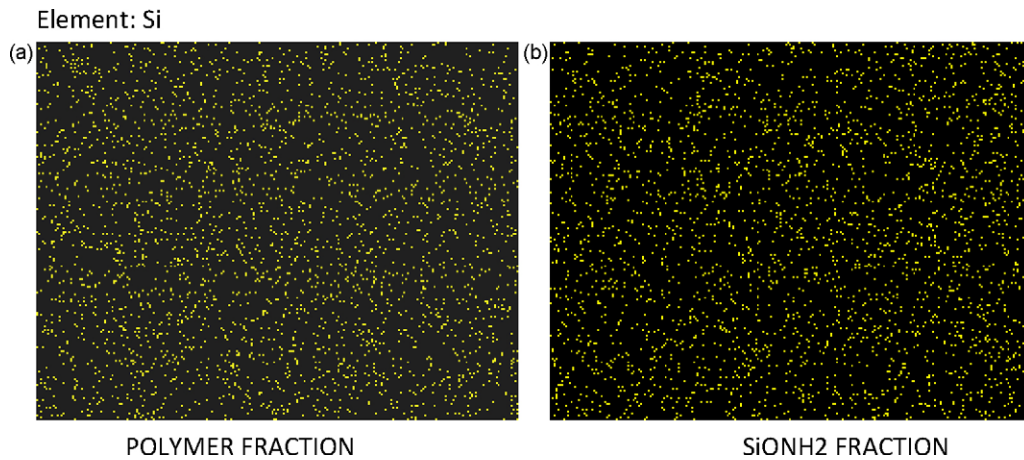


Fig. 6. EDX mapping onto polymer fraction(a) and silica fraction (b) of SIONH-D sample.

composite membranes and pristine polymer used as a reference [21], as reported in Figs. 9 and 10.

At 80 °C the composite membranes performance follows the same trend of proton conductivity and the best performance is reached by using H₂SO₄ as the last treatment (B and D).

The A-treated composite membrane shows lower performance than pristine membrane and this is in accordance with the proton conductivity values (0.027 S cm⁻¹ and 0.14 S cm⁻¹ for composite and pristine, respectively).

For sample C the low performance could be explained by considering the low OCV values (0.785 V) and high cell resistance (0.72 Ω cm²) due to the post-casting treatment. For the other samples (B and D) the performance of pristine polymer were reached despite the lower proton conductivity, meaning that the structural and morphological properties due to H₂SO₄ treatment as last step is favourable for fuel cell operation.

At high temperature (120 °C), where the swelling process should be enhanced, all composite membranes show higher performance than pure s-PEEK membrane, due to silica introduction that limits the swelling effect.

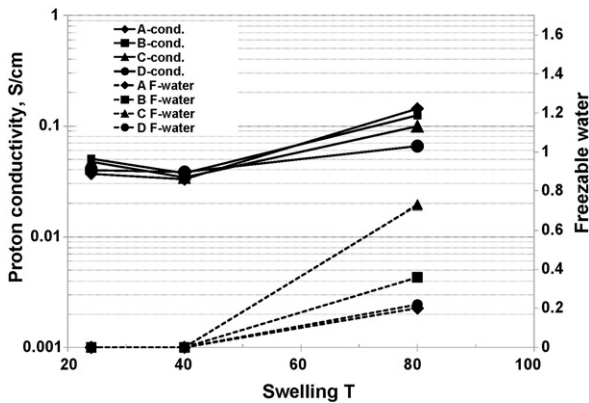


Fig. 7. Proton conductivity and freezable water behaviour of pristine membranes as a function of swelling temperature.

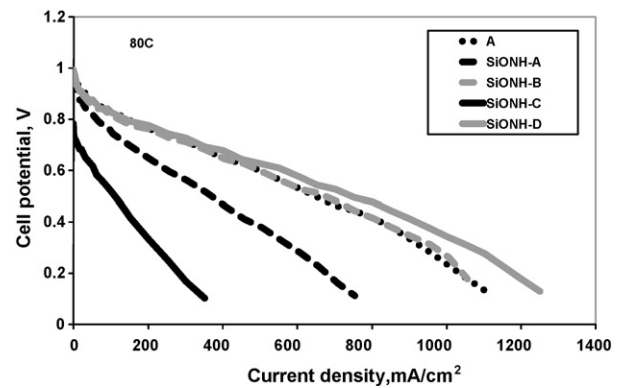


Fig. 9. Polarisation curves comparison at 80 °C for composite and pristine membranes.

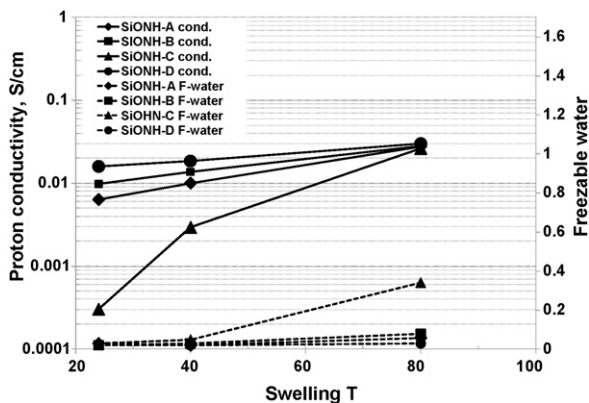


Fig. 8. Proton conductivity and freezable water behaviour of composite membranes as a function of swelling temperature.

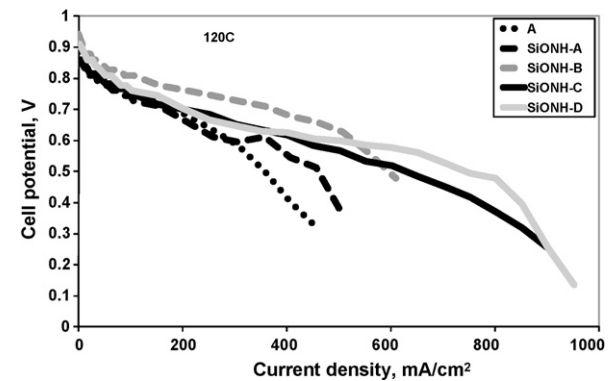


Fig. 10. Polarisation curves comparison at 120 °C for composite and pristine membranes.

The A-treated composite membrane reaches similar performance than pristine membrane, even if cell resistance values of 0.36 and 0.12 Ωcm^2 were recorded, respectively. This behaviour could be attributed to silica introduction that presumably reduces the amount of F water into the membrane at this temperature and maintains suitable properties for fuel cell operation.

C-composite sample shows better performance increasing the temperature from 80 °C to 120 °C. However, taking into account the effect of post-casting treatment that destabilises the polymer matrix and breaks the polymer–silica interactions, a low stability in terms of mechanical properties can be expected with a consequent fuel cell performance failure with the time.

For composite samples B and D that underwent H_2SO_4 as last treatment, the performance is improved confirming the appropriate structural and morphological properties due to acid treatment as discussed at 80 °C. Moreover the annealing (D) favours the limiting current enhancement due to a strengthening of membrane structure that improves the contact between membrane and electrodes in the MEA.

4. Conclusions

In s-PEEK membranes it is possible to control and enhance the membrane performance only by a simple and easy post-casting treatment. DSC measurements revealed that the amount of UF water depends on the adopted treatment and is higher than F one at a swelling temperature of 80 °C. For composite s-PEEK–SiONH₂ membranes, the total amount of water is lower than that for pristine membranes due to interactions between NH₂–SO₃H groups that reduces the polymer capability to coordinate water. The F water is already present when the w.u. is effected at $T < 80$ °C, due to the silica presence that readily incorporates water in a phase free to freeze. At $T > 80$ °C, the F water content is related to the post-casting treatments.

The structural analyses showed that while the treatments do not change the crystalline phase in pristine polymers, they modify the composite membranes.

Morphological measurements highlighted that silica is uniformly dispersed into the polymeric matrix at the micro-scale, for all the considered post-casting treatment. However at the macroscale different size of silica agglomerates are influenced by the treatment as evidenced by Laser measurements.

Pristine s-PEEK membranes proton conductivity increases by increasing the temperature and reaches the highest values when F water is present, while the proton conductivity of composite samples is lower than pristine samples. The proton conductivity of composite membranes is both influenced by the treatments and the silica presence.

Fuel cell tests at 80 °C revealed that the performance of composite membranes rank according to the value of proton conductivity and the best performance is reached by using H_2SO_4 as the last treatment (B and D). At 120 °C, where the swelling process should be enhanced, all composite membranes show higher performance than pure s-PEEK membrane, due to silica introduction that limits the swelling effect. Moreover, when annealing is processed before acid treatment, a strengthening of the membrane structure is obtained improving the contact between the membrane and the electrodes inside the MEA. As a result, the limiting current is increased.

References

- [1] D.J. Jones, J. Roziere, in: W. Vielstich, A. Lamm, H. Gasteiger (Eds.), *Handbook of Fuel Cell Technology*, Wiley & Sons, London, 2003, pp. 447–455.
- [2] G. Alberti, M. Casciola, in: K.D. Kreuer, D.R. Clarke, M. Rühle, J.C. Bravman (Eds.), *Annual Review of Material Research*, vol. 33, 2003, pp. 129–154.
- [3] D.J. Jones, J. Roziere, *J. Membr. Sci.* 185 (2001) 41–58.
- [4] K.D. Kreuer, in: W. Vielstich, A. Lamm, H. Gasteiger (Eds.), *Handbook of Fuel Cell Technology*, Wiley & Sons, London, 2003, pp. 420–435.
- [5] E. Cho, J. Park, S. Park, Y. Choi, T. Yang, Y. Yoon, C. Kim, W. Lee, S. Park, *J. Membr. Sci.* 318 (2008) 355–362.
- [6] G. Alberti, M. Casciola, L. Massinelli, B. Bauer, *J. Membr. Sci.* 185 (2001) 73–81.
- [7] Y. Gao, G.P. Robertson, M.D. Guiver, X. Jian, S.D. Mikhailenko, S. Kaliaguine, *Solid State Ionics* 176 (2005) 409–415.
- [8] K.D. Kreuer, *Solid State Ionics* 97 (1997) 1–15.
- [9] A.F. Ismail, N.H. Othman, A. Mustafa, *J. Membr. Sci.* 329 (2009) 18–29.
- [10] E. Sengul, H. Erdener, R.G. Akay, H. Yuçel, N. Bac, I. Eroglu, *Int. J. Hydrogen Energy* 34 (2009) 4645–4652.
- [11] G. Qijun, W. Yuxin, X. Li, W. Guoquiang, W. Zhitao, *Chin. J. Chem. Eng.* 17, 2 (2009) 207–213.
- [12] J. Jaafar, A.F. Ismail, T. Matsuura, *J. Membr. Sci.* 345 (2009) 119–127.
- [13] A. Carbone, R. Pedicini, G. Portale, A. Longo, L. D'Ilario, E. Passalacqua, *J. Power Sources* 163/1 (2006) 18–26.
- [14] A.K. Sahu, P. Pitchumani, P. Sridhar, K. Shukla, *Bull. Mater. Sci.* 3 (2009) 285–294.
- [15] A.K. Sahu, G. Selvarani, P. Pitchumani, P. Sridhar, A.K. Shukla, *J. Appl. Electrochem.* 37 (2007) 913–919.
- [16] F. Mura, R.F. Silva, A. Pozio, *Electrochim. Acta* 52 (2007) 5824–5828.
- [17] A. Saccà, I. Gatto, A. Carbone, R. Pedicini, E. Passalacqua, *J. Power Sources* 163 (2006) 47–51.
- [18] A. Saccà, A. Carbone, E. Passalacqua, A. D'Epifanio, S. Licocchia, E. Traversa, E. Sala, F. Traini, R. Ornelas, *J. Power Sources* 152 (2005) 16–21.
- [19] A. Carbone, A. Saccà, I. Gatto, R. Pedicini, E. Passalacqua, *Int. J. Hydrogen Energy* 33 (2008) 3153–3158.
- [20] J. Kerres, W. Cui, Patent US 6,300,381 B1 (2001).
- [21] A. Carbone, R. Pedicini, A. Saccà, I. Gatto, E. Passalacqua, *J. Power Sources* 178 (2008) 661–666.
- [22] I. Gatto, A. Saccà, A. Carbone, R. Pedicini, F. Urbani, E. Passalacqua, *J. Power Sources* 171 (2007) 540–545.
- [23] S. Swier, Y.S. Chun, J. Gasa, M.T. Shaw, R.A. Weiss, *Polym. Eng. Sci.* 45 (2005) 1081.
- [24] K. Ishikiriyama, M. Todoki, *Thermochim. Acta* 256 (1995) 213–226.
- [25] P. Krishnan, J.S. Park, C.S. Kim, *J. Membr. Sci.* 279 (2006) 220.
- [26] B.B. Sauer, B.S. Hsiao, *Polymer* 34 (1993) 3315.